UMYU Scientifica, Vol. 4 NO. 1, March 2025, Pp 396 – 407
https://doi.org/10.56919/usci.2541.040
ISSN: 2955 – 1145 (print); 2955 – 1153 (online)
*A periodical of the Faculty of Natural and Applied Sciences, UMYU, Katsina*

ORIGINAL RESEARCH ARTICLE

# GIS-Based Determination of Urban Heat Island Profile of Kaduna Metropolis, Nigeria

*[1]Ahmad Hamza Abdullahi, [1]Abdulrazak Ahmed, [2]Jamilu Usman, [1]Abdulhakim Hassan Wagini, [3]Yunusa Halliru, [4]Saliu Ibrahim Ajobunu, and [4]Zainab Yusuf

[1]Department of Geography and Environmental Management, Ahmadu Bello University, Zaria, Kaduna, Nigeria
[2]Department of Geography, Gombe State University, Gombe, Nigeria
[3]China Institute of Water Resources and Hydrology (IWHR), China
[4]Department of Environmental Management, Kaduna State University, Kaduna, Nigeria

## ABSTRACT

Studies on Urban Heat Island (UHI) have become an important way to create sustainable and lively cities; it improves public health and enhances urban quality of life. An increase in the level of Land Surface Temperature (LST) and a corresponding rise in the urban temperature as UHI among many cities of Nigeria brings about more outbreaks of heat related diseases. The current research focused on the assessment of spatial patterns of LST and UHI in the Kaduna metropolis. Land sat 8, operational land imager (OLI) imagery of April 2024 was used for the research. Analysis was conducted through the determination of the Normalized Difference Vegetation Index (NDVI), vegetation density map, satellite brightness temperature, LST, and finally, UHI profile on ArcGIS 10.8 software. Results on vegetation density revealed that areas with very low vegetation cover recorded the highest (44.86%) while those with moderate vegetation cover had the lowest (12.06%). The findings also indicated that the highest (47.55%) percent of the study area experienced higher LST while only 8.93% experienced lower LST. Results also show that most (37.43%) percent of the research area recorded a high (6.55°C) rate of UHI, 16.38% recorded about 8.5°C, while only 1.87% experienced a low UHI of 3.4°C. Results of the regression analysis between NDVI and UHI indicated an inverse relationship between vegetation density and urban heat islands in such a way that, for every 1-unit increase in vegetation density, UHI decreases by ~19.63 units while the negative sign means more vegetation resulted in lower urban heat (cooling effect). In conclusion, the study indicated that the western and heart of the metropolis had high UHI profiles while the eastern part of the area and other areas along the water bodies experienced lower UHI. Based on these, the study recommends the provision of strategies such as plating trees which will help in reducing higher rate of heat, this is more especially during the hot and dry season.

## ARTICLE HISTORY

Received December 20, 2024
Accepted March 28, 2025
Published March 31, 2025

## KEYWORDS

NDVI, Urban, Heat, Island and Profile



## INTRODUCTION

Urban Heat Island (UHI) is simply referred to as the contrast in atmospheric or surface temperature between the urban areas and their surrounding suburbs. It can basically be divided into Canopy Layer Heat Island (CLHI); Boundary Layer Heat Island (BLHI), and Surface Heat Island (SHI). While CLHI and BLHI describe the pattern of urban atmospheric warming at varying altitudes above the ground, SHI describes the ground-level warming (Fabrizi et al., 2010). The CLHI is typically detected by ground stations using thermometers to measure air temperature in the canopy layer. On the other hand, satellite imageries, which capture the spatial patterns of upwelling thermal radiance through remote sensing technology, are used to estimate Land Surface Temperature (LST). From that, the SHI is deduced (Ogashwar and Basto, 2012). Environmentalists and other research personnel can use Land surface temperature to derive a lot of information about the surface physical properties and climate, which plays a role in many environmental processes. Therefore, LST served as an input parameter to monitor the rapid and recurrent changes in the global environment; it plays a key role in modeling the surface energy balance and has a substantial

**Correspondence:** Ahmad Hamza Abdullahi. Department of Geography and Environmental Management, Ahmadu Bello University, Zaria, Kaduna, Nigeria. ✉ ahmadhamzaabdul@gmail.com.
**How to cite**: Abdullahi, A. H., Ahmed, A., Usman, J., Hassan, A. W., Halliru, Y., Saliu, A. I., & Yusuf, Z. (2025). GIS-Based Determination of Urban Heat Island Profile of Kaduna Metropolis, Nigeria. *UMYU Scientifica*, 4(1), 396 – 407. https://doi.org/10.56919/usci.2541.040

impact on analyzing other heat-related issues such as soil moisture, evapotranspiration and urban heat islands.

Remote sensing (RS) can be described as an art, science, and technology for the acquisition of data pertaining to the earth's surface using sensors from space platforms According to Curran and Atkinson (1998), RS are a collection of tools used to increase understanding of our environment in space and time. It is an extensive tool and technique used to capture the characteristics of the physical environment without onsite observation, becoming a tool to reckon with in evaluating and monitoring environmental and ecological processes. Remote Sensing (RS) and GIS are combination of tools that provide a strong framework for studying UHI. They offer uncountable advantages during data collection, processing, analysis, visualization, and decision-making processes. The tools allow for real-time monitoring and management of UHIs. They support the development of models for the prediction of future effects of UHI based on urban growth and climate change under different conditions. However, there are a lot of remote sensing data ranging from land observation to meteorological ones such as Modis, NOAA-17/AVHRR, and Meteosat-9 (Jacob, 2015) for estimating LST. However, Landsat is the most used satellite that provides thermal data using just one long wave infrared (LWIR) band, with a higher spatial resolution (NASA 2015). Because it has a relatively high spatial resolution, therefore, a more detailed land surface temperature pattern can be obtained, which makes it possible to study the relationship between land surface temperature and different land use /land cover types (LULC) and enables the detection of single sources of the highest heat emission (Jacob, 2015).

Many cities and metropolitan areas, including the Kaduna metropolis, suffered from spatial and temporal variation of LULC mainly due to population increase, which reduces vegetation cover that is an important factor in providing suitable habitat for many species, controlling atmospheric $CO_2$ content, and regulating climate. Hence an increase heat emission in the area, consequently affecting public health. One of the ways that help in addressing issues of that nature includes the determination of the urban heat island profile, which the current study looks into. Urban heat island (UHI) profile simply means the distribution pattern of temperature variations between urban and suburban areas (Oke et al., 2020). Studies were previously conducted to investigate the pattern and intensity of LST and UHI in some major cities of the world, such as the studies conducted by Ngie et al. (2015), who estimate Land Surface Temperatures from Landsat ETM+ images for Durban, South Africa. Abuloye et al. (2015) also assess the daytime surface urban heat island in Onitsha, Nigeria. In addition, Babalola and Akinsanola (2016) studied change detection in Land Surface Temperature and Land Use Land Cover in metropolitan Lagos. Others such as Wuyep and Samuel (2020) in Jos, Nigeria; Oke et al. (2020); Akbari et al. (2021) and Changkuan et al. (2025) in Northeast China Plain (NCP), Huang-Huai-Hai Plain (HHP), Qinghai Tibet Plateau (QTP), and Loess Plateau (LP) studied pattern of UHI and its relationship with vegetation density in their study areas. In the Kaduna metropolis, Zahraddeen et al. (2016) estimated the land surface temperature of the area using Landsat images. The title of Mande and Abashiya's (2020) work was to assess the urban heat island of Kaduna metropolis. However, Mande, Abashiya, and other researches in Kaduna metropolis failed to examine the profile of the UHI in the metropolis, which is an important factor that deteriorates air quality and increases human health risk. Therefore, the focus of this study was examining the pattern of urban heat island profile in relation to the density of vegetation in the Kaduna metropolis using RS and GIS technologies.

## MATERIALS AND METHODS

### Study Area

The study area (Kaduna metropolis) is located between Latitudes 10° 26' 00" North and 10°38' 00" North of the Equator and Longitudes 7° 21' 00" East and 7° 33' 00" East of the Greenwich Meridian (Figure 1).

Kaduna metropolis and Kaduna state is climatic characteristics are predominantly tropical wet and dry, coded as Aw according to Koppen's classification. The temperature of the area is generally high throughout the year, but there are some seasonal changes. The rainy season begins in April and lasts till October, while the dry season (harmattan) spans from November to March (Bello, 1993). Nigerian Meteorological Agency (NIMET) (2018) reported that the maximum temperature in Kaduna metropolis is above 30oC, while the hottest months are from March to May.

### Methods of Data Collection

The satellite imagery used for the study was the Land sat Operational Land Imager (OLI) of April 2024 with a spatial resolution of 30m. This data has been used because April is the hottest month in the state, and 2024 is the most recent year. This type of imagery has been chosen because it was found to be significant in the study of environmental change detection and thermal studies. Band 4, 5, and 10 and meta data file of the imagery were downloaded from the United State Geological Survey (USGS). The imagery used in this study does not undergo preprocessing activities such as geo-reference, radiometric, and geometric correction because it was orthorectified by the USGS center before download (USGS, 2016).

### Methods of Data Analysis

To arrive at the desire results, analysis was conducted in ArcGIS 10.8 environment, and the classification of maps was done using Jenks classification method through the following processes:

### Generation of NDVI imagery

NDVI (appendix 1) imagery for this study was first generated using the formula in equation 1. This served as input data for determining fractional vegetation cover (PV) of the area as a vegetation density map using

equation 2. Band 5 of the data serves as the near-infrared band, while band 4 serves as the red band.

$$NDVI = \frac{Nearinfrared - Red}{Nearinfrared + Red} \quad \text{Eq 1}$$

$$PV = \left(\frac{(NDVI - NDVImin)}{(NDVImax - NDVImin)}\right)^2 \quad \text{Eq 2}$$

**Land surface temperature retrieval**

Land surface temperature was derived from thermal infrared (TIR) band 10. The raw digital numbers (DNs) were first converted to spectral radiance (Lλ) using equation 3 as obtained from Landsat user's handbook (NASA, 2015). However, the formula in equation 4 has been used to convert spectral radiance to satellite brightness temperature called black body temperature (TB). While the final land surface temperature is estimated using the mono window equation as presented in equation 5.

$$L\lambda = \frac{(Lmax - Lmin)}{(Qcalmax - Qcalmin)}(Qcal - Qcalmin) + Lmin \quad \text{Eq 3}$$

Where:
Lλ: Spectral radiance (W·m−2−2·sr−1−1·μm−1−1)
Lmax and *L*min: Maximum and minimum spectral radiance values
Qcalmax and *Q*calmin: Maximum and minimum quantized calibration pixel values
Qcal: Quantized calibrated pixel value (DN)

$$TB = \frac{k2}{\ln\left(\frac{k1}{L\lambda} + 1\right)} - 272.3 \quad \text{Eq 4}$$

Where:TB: Brightness temperature (in Kelvin)
K1 and K2: Thermal calibration constants

$$LST = \frac{TB}{1 + (\lambda * \frac{TB}{P})\ln(e)} \quad \text{Eq 5}$$

Where: λ: Wavelength of emitted radiance (11.5 μm for Landsat 8 Band 10)
ϱ=h·c/σϱ=*h*·*c*/*σ* (1.438 × 10−2−2 m·K), where h*h* is Planck's constant, c*c* is the speed of light, and σσ is the Stefan-Boltzmann constant

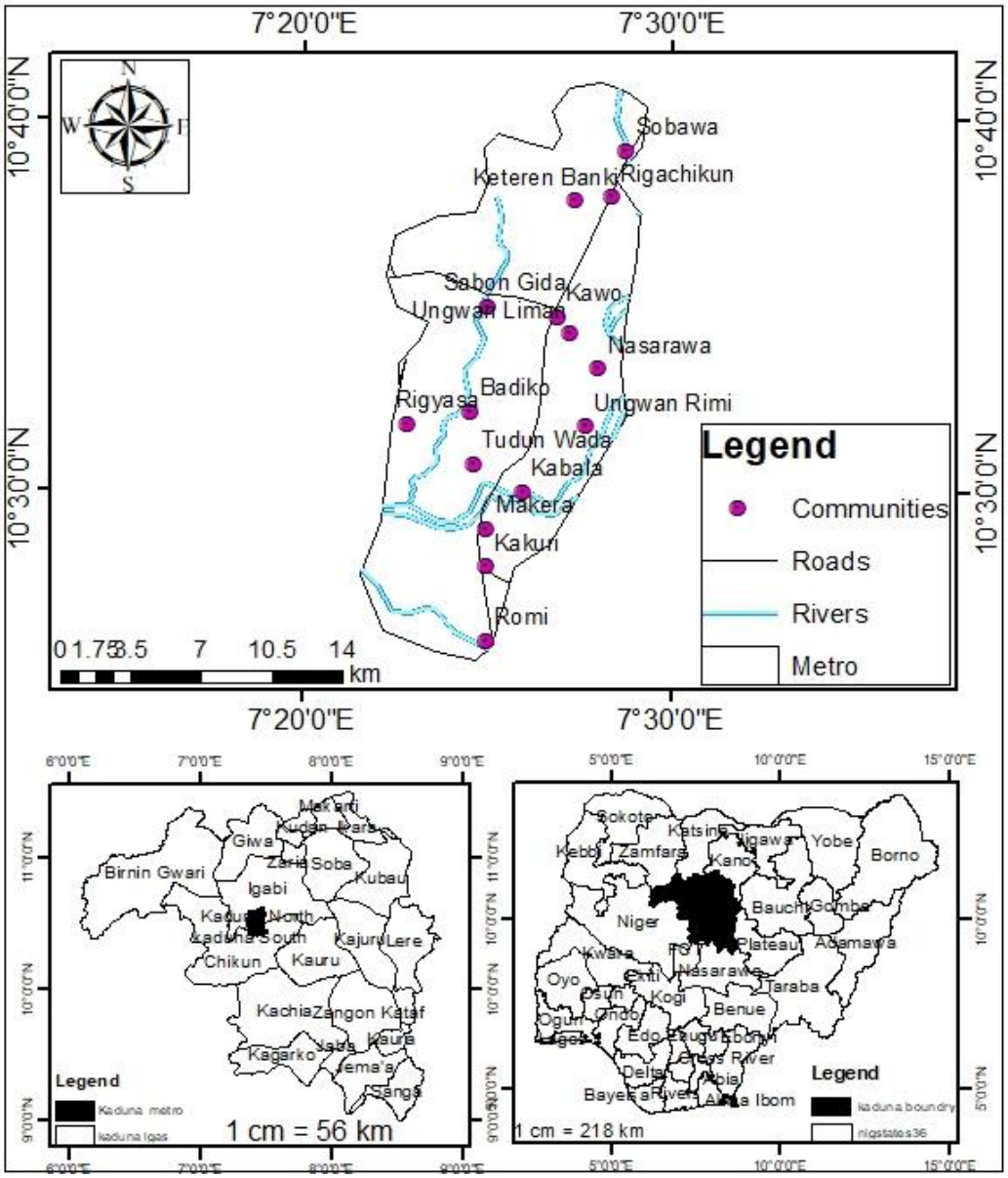


**Figure 1: Map of the Study Area**
**Source: Adapted from Administrative Map of Kaduna State**

### Determination of urban heat island profile

UHI profile was finally determined based on the formula in equation 5, while the stack profile was formed using a functional surface tool under 3D analyst tools.

$$UHI = \frac{LST - LSTmean}{\text{Standard Deviation}} \quad \text{..... Eq 6}$$

### Comparison between NDVI and UHI

The researchers created 60 random points (appendix 2) based on 1 sample point per 4 KM². These points were used to extract the values of NDVI and UHI using extract values to point. The Ordinary Least Squares (OLS) regression was applied to the extracted values in the ArcGIS 10.8 environment to perform regression analysis. In order to ascertain the level at which the variables are related. Before running the model, the researcher assumed that residuals are homoscedastic, independently, and identically distributed normally around a mean of zero. The tool was used to analyses the direct influence of vegetation density on the distribution of UHI in the area. The tool is located in the modeling spatial relationship sub-menu of spatial statistics tools and is used to generate an output feature class in the form of color ramp map and tables containing coefficient information and diagnostics. The output diagnostics parameters include the Akaike Information Criterion (AICc), Coefficient of intercept, Coefficient of Determination, Joint F statistic, Wald statistic, Koenker's Breusch-Pagan statistic, Jarque-Bera statistic, Sigma-squared values, corrected and uncorrected AICc. The result of the OLS analyses was presented in the form of a table, while interpretations and discussions were done based on R-squared, Jarque-Bera Statistic, t-statistic, and Coefficient of intercept.

### Validation of the findings

After the analysis, findings were validated through ground truthing. During the process record of air temperature (AT) across the 60 sample points was taken in the time and compared with that of LST. It was discovered that the values of LST for 97% of the sample points exceed that of AT by 0.4 to 0.9. In addition, the researchers realized that there are higher AT values in the core part of the metropolis than what is obtained along the suburb of the study area, which indicated the validity of the results that UHI has been lower in the peri-urban area and water bodies when compared with the core of the city. AT has been used because, it has been positively correlated with LST only that LST is higher than AT during daytime and less than during night.

## RESULT AND DISCUSSION

### Vegetation Density

The results in Figure 2 and Table 1 show the vegetation density of the research area. Table 1 revealed that 44.86% of the area was occupied by very low vegetation while only 12.06% had moderate vegetation cover. The moderate pattern of vegetation cover is mainly found along water bodies and in the northern part of the study area around Ketaran Banki. This might be associated with the fact that; the study area is a city with more buildup than any other form of land use – land cover (appendix 3). In fact, the result indicated that areas with the highest density of vegetation are those without buildings. The implication of this in relation to the research is that the area is expected to be affected by high land surface temperature and urban heat island, which will consequently might lead to a high rate of heat-related diseases and loss of both surface and underground water. The result is in line with that of Cyril et al. (2019) in Kaduna South Local Government Area, who reported an increased built-up area by 32.7% from 1987 to 2016 and a decrease in vegetation cover within the study period. This finding also supports Nantip et al. (2023) that there is a gradual increase in built up area in Kaduna metropolis from 1990 to 2018 and a decline in vegetation cover by about 28.2%.

### Distribution of Land Surface Temperature (LST)

The visual pattern of the LST ranging from 28.42°C to 31.91°C in Figure 3 and the values in Table 1 showed that the southern part of the study area appeared warmer, which might be attributed to the fact that the southern part was more built-up and contained very low vegetation density as shown in Figure 2. The result in Table 1 shows that the highest (47.55%) of the research area recorded high LST while the lowest (8.93%) percent recorded low LST. The finding further indicated that places occupied by rivers recorded the lowest (less than 30°C) LST while the built-up areas recorded above 30.5°C. This pattern is associated with the fact that water bodies do not reflect solar radiation; hence, the surface of the water will be cooler than the surrounding environment, which reflects back energy received from the Sun. In view of this, the finding clearly indicated how urban development, such as buildings, industrial, and other construction activities, increase the rate of surface temperature through non-evaporating and non-transpiring surfaces.

The findings further revealed the consequences of removing vegetation cover for urban development, which generally raises the surface radiant energy. The finding is in line with that of Falahatkar et al. (2011) in Isfahan, where bare land and farmland recorded the highest values of land surface temperature. This also supports Mande and Abashiya (2020) in the Kaduna metropolis, who attributed the increase in LST of the metropolis to the development in construction activities. The results are also in line with Abdullahi (2020), who reported an increase in the LST of Kano metropolis from 1986 to 2018, with the highest (37.65oC) mean value in the north and south. This result is also in agreement with that of Zahraddeen et al. (2016), who revealed the highest mean value of LST in 2015 than 2009 and 2006 in the Kaduna metropolis. The results are also in line with that of Yusuf et al. (2023) in Nguru of Yobe State, which reveal the highest (39.39°C) LST in the northern part of the study area and the lowest (22.33°C) in the southern part of the area. Despite non-numerical assessment, the researchers stated the variation in the LST to have brought about variation in the UHI of the area.

**Urban Heat Island Profile**

The results in Figure 4 and Table 2 present the findings on UHI in the research area. The largest part of the Kaduna metropolis experiences optimal thermal conditions for living. These areas have UHI above 6.14, which might be linked to their high built-up and locations in close proximity to the bare land. However, the areas that are hit by lower UHI effects happen to be small pocket areas of the Kaduna metropolis; these areas are located on the surface water and those with similar characteristics. Figure 5, on the other hand, shows the profile of the UHI in the area; the result indicated how the rate of the urban heat was fluctuating with the distance from one land use – land cover and another. Since, the profile was drawn from the western part of the study area through the heart of the metropolis to the extreme eastern region.

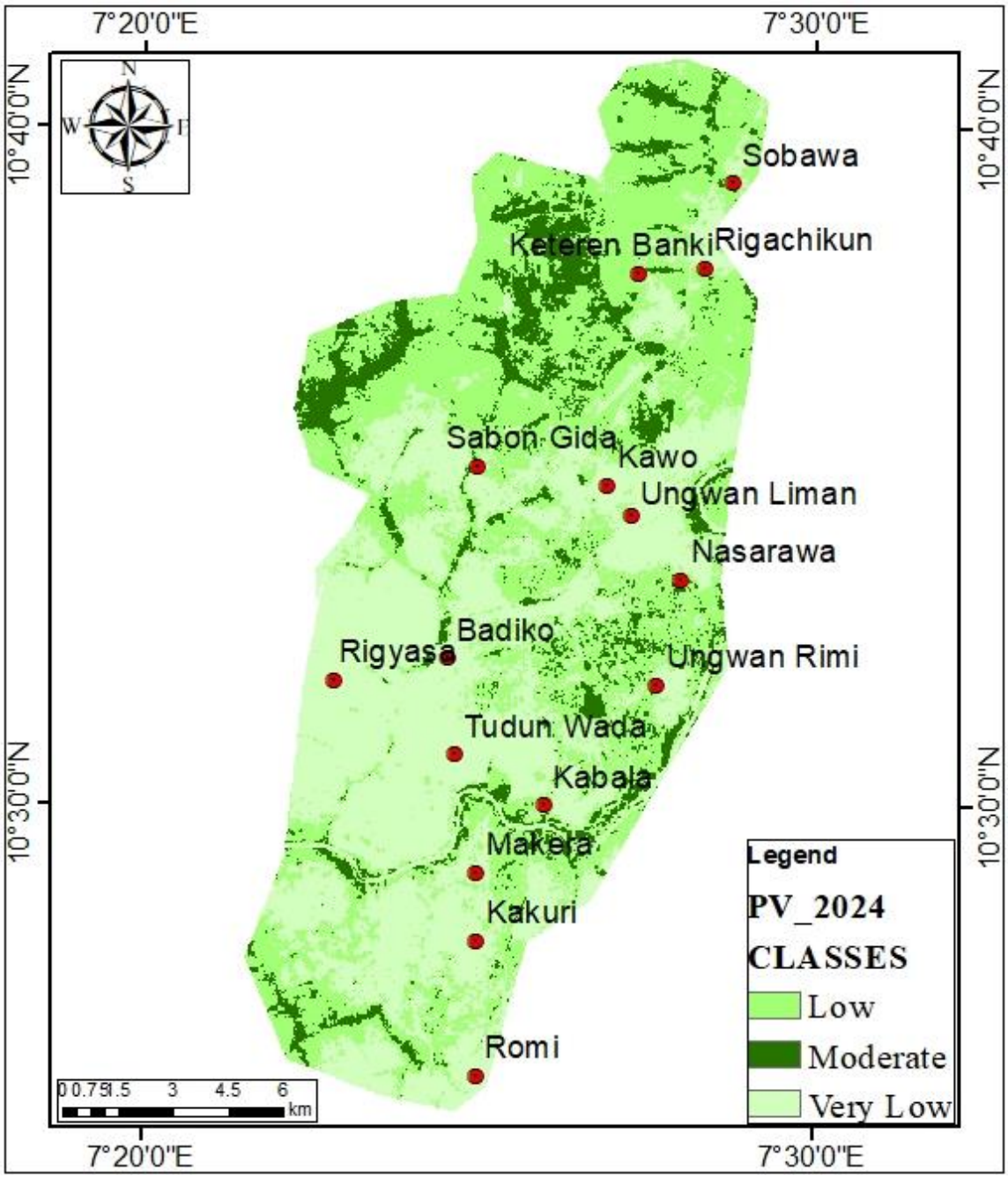


**Figure 2: Vegetation Density Map**

**Table 1: Vegetation Density and Land Surface Temperature**

| | **Vegetation Density** | | | **Land Surface Temperature (°C)** | |
|---|---|---|---|---|---|
| Classes | Area [km²] | % | Classes | Area [km²] | % |
| Moderate | 30.06 | 12.06 | High | 118.51 | 47.55 |
| Low | 107.37 | 43.08 | Moderate | 108.49 | 43.53 |
| Very low | 111.82 | 44.86 | Low | 22.25 | 8.93 |
| **Total** | **249.25** | **100.00** | **Total** | **249.25** | **100.00** |

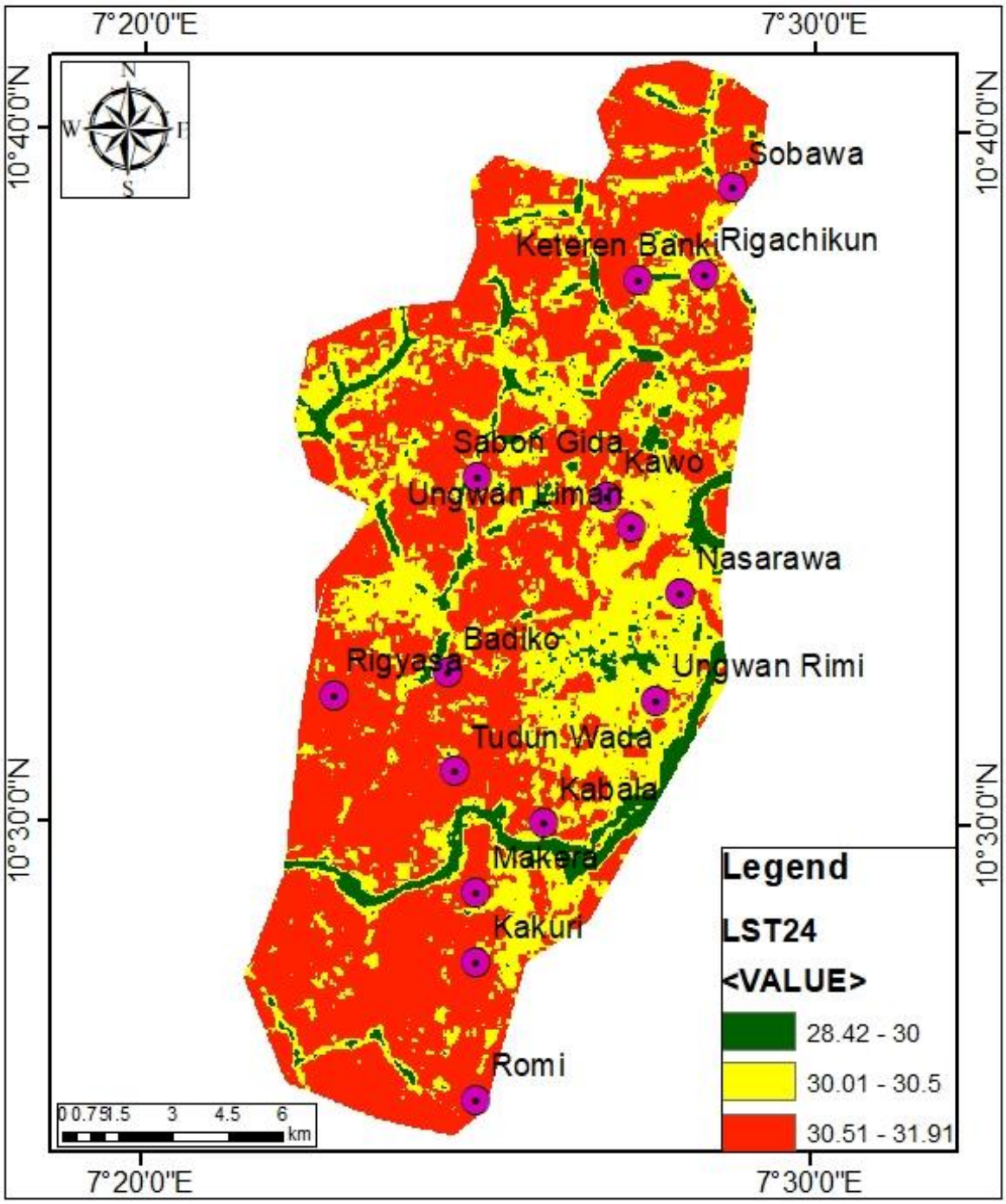


**Figure 3: Land Surface Temperature Map**

**Table 2: Urban Heat Island**

| Classes | Average UHI (°C) | Area [km²] | % |
|---|---|---|---|
| Very high | 8.5 | 40.83 | 16.38 |
| High | 6.55 | 93.29 | 37.43 |
| Moderate | 5.71 | 74.21 | 29.77 |
| Low | 4.61 | 32.39 | 12.99 |
| Very low | 1.87 | 8.53 | 3.42 |
| **Total** | | **249.25** | **100.00** |

**Table 3: NDVI Versus UHI**

| Variable | Coefficient [a] | t-Statistic | Probability [b] | Robust_SE | Pr [b] |
|---|---|---|---|---|---|
| **Intercept** | 7.575182 | 24.503315 | 0.000000* | 0.261435 | 0.000000* |
| **NDVI** | -19.626166 | -4.691486 | 0.000029* | 3.469015 | 0.000001* |
| Multiple R-Squared [d]: | 0.343853 | Adjusted R-Squared [d]: | 0.328230 | | |
| Jarque-Bera Statistic [g]: | 2.687129 | Prob(>chi-squared), (2) degrees of freedom: | 0.260914 | | |

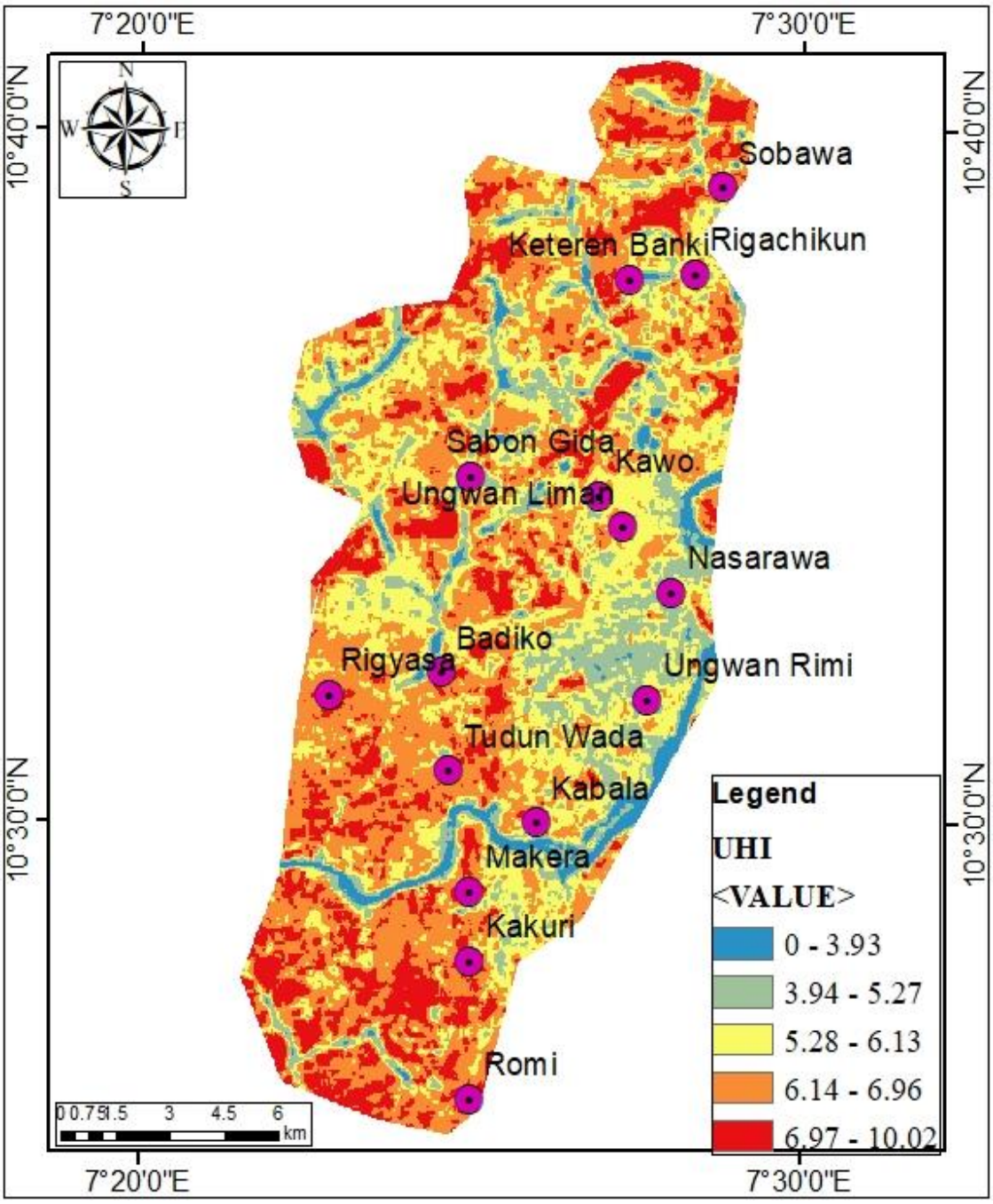


**Figure 4: Urban Heat Island**

The results indicated that there is more heat in the western part and heart of the city than in the eastern part. This result might be linked to the concentration of buildings in the west and central parts, and appearance of River Kaduna in the eastern part, or the existence of vegetation cover. The research findings were in line with the statement of Ifatimehin (2007) that UHI is more at the heart of a city where there is the concentration of buildings and reduces as one moves outward. These results correspond with that of Isioye et al. (2020), who observed that 40% of the Abuja area council experiences a worse UHI effect. The researchers also reported the city's suburb part to be ecologically more comfortable than the heart part. The finding further proves how the absence of surface water and vegetation cover, especially in urban centers where population and industrial activities are high, brings about an increase in the level of UHI. This result also supports Zahraddeen et al. (2016), who recorded a a strong negative correlation between NDVI and LST in Kaduna Metropolis. In view of these, the researcher concluded that there is high UHI in the heart of Kaduna metropolis and low along water bodies.

### NDVI Versus UHI

Results of the regression analysis between NDVI and UHI are presented in Table 3. Results from the Coefficient ($\beta_0$) at 7.575 indicates that when NDVI = 0 (no vegetation), the expected UHI value is 7.575 units. The slope of the Coefficient ($\beta_1$): -19.626, on the other hand, implied that for every 1-unit increase in NDVI, UHI decreases by ~19.63 units, while the negative sign means more vegetation resulted in lower urban heat (cooling effect). Hence, the findings indicated an inverse relationship between vegetation cover and urban heat islands in the

study area. Moreover, results on t-Statistic = 24.50, p < 0.000* implied a highly significant relationship between the variables. However, the multiple R-squared (0.344) model explains 34.4% of the variance in UHI due to vegetation cover, suggesting a moderate relationship between NDVI and UHI. Jarque-Bera Test (p = 0.261) shows a normal distribution of the residuals (p > 0.05), and so satisfies OLS assumptions. In general, the findings show that although vegetation cover is a determinant to the level of UHI, in the study area there are other factors such as the nature of buildings and the the presence of surface water, that play a major role. This was evidently presented in Figures 4 and 5, whereby places close to water bodies recorded lower UHI while those in the core of the metropolis recorded the highest value of UHI.

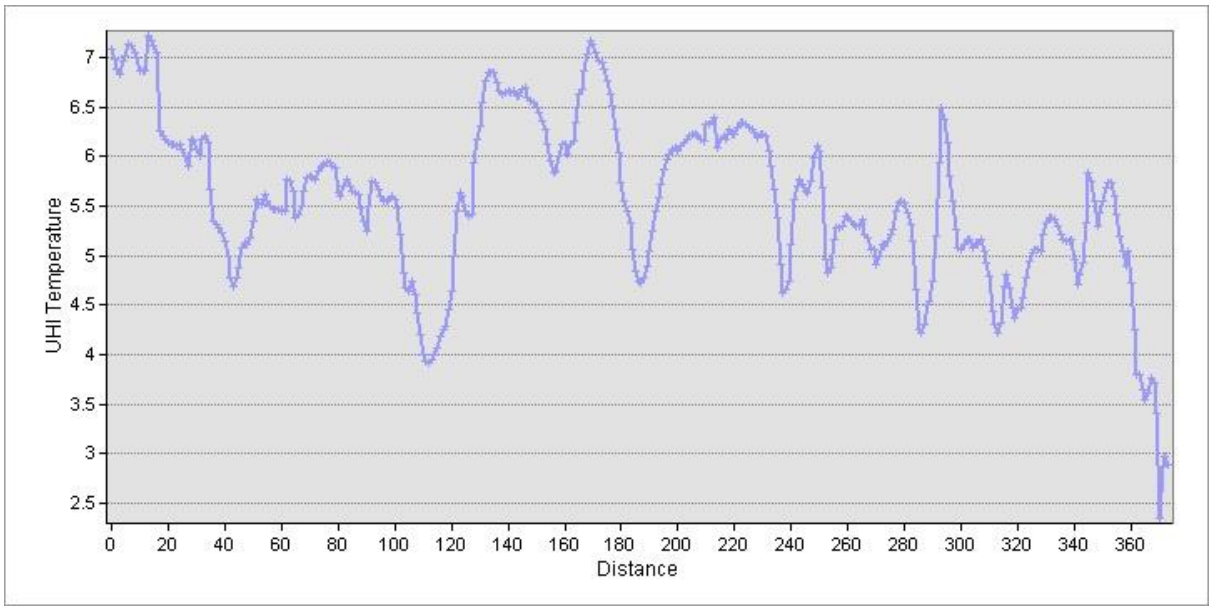


**Figure 5: Urban Heat Island Profile**

The results correspond with that of Adewara and Oyewole (2019) in Ilaro, Ogun state, which showed that thick forest and light vegetation zones recorded lowest UHI throughout the study years while built up and bare surfaces had the worst UHI level. Findings from the current study correspond with that of Wuyep and Samuel (2020) in Jos, which reported a decrease in urban heat island from an average of 29.52°C in the city center occupied by built-up to 25.11°C in vegetated areas and 20.61°C along water bodies mainly to the North and North-East of the metropolis. Results from this study also conform with that of Changkuan et al. (2025) in Northeast China Plain (NCP), Huang-Huai-Hai Plain (HHP), Qinghai Tibet Plateau (QTP), and Loess Plateau (LP). The result reported that for every 1 % increase in the proportion of unused land area, the LST decreased by 0.250 °C. The finding also shows the warming effect of construction activities on LST, with LST increasing by 0.079 °C to 0.338 °C for every 1 % increase in the proportion of construction area. The results support Oke et al. (2020), who stated that higher temperatures in urban zones have been related to human activities, reduced vegetation, and the prevalence of heat-absorbing materials like concrete and asphalt. Findings from this study also support Akbari et al. (2021) that increasing urban greenery, implementing cool roofs and pavements, and promoting energy-efficient building designs significantly serve as mitigation strategies to reduce UHI intensity.

## CONCLUSION AND RECOMMENDATIONS

Detail information on the distribution of urban heat islands in most parts of Nigeria, including Kaduna metropolis, is lacking due to the problems of discrete data provided by field studies and the absence of its record on metrological stations, but with the use of satellite remote sensing coupled with GIS an effective methodology for extracting this information is provided. In this research, land sat imagery helps to analyze the Spatial and temporal pattern of LST and UHI in the research area. In conclusion, the finding of this study revealed that the largest (47.55%) part of the study area recorded higher LST while the lowest (8.93%) part of the study area recorded low LST. The study also concluded that 37.43% of the area recorded high (6.55°C) UHI, while only 1.87% recorded 3.42°C UHI. In view of this finding, the study recommended the use of modern technologies to identify areas that required additional protection against the negative consequences of excessive heat in Kaduna metropolis and Nigeria as a whole. Based on the findings from this study, the research recommends adopting methods such as provision of shading spaces, implementing and enforcing green building standards in our urban areas as mitigation strategies for the effects of UHI.

## REFERENCES

Abdullahi, A. H. (2020). GIS-based analysis of the relationship between urban vegetation and land surface temperature of Kano metropolis, Nigeria. In A. F. Abdussalam, A. A. Adepetu, & I. Zaharaddeen (Eds.), *Ecosystem dynamics and disaster risk management*. M. O. Press and Publishers Ltd.

Abuloye, A. P., Popola, K. S., Adewale, A. O., Onana, V. E., & Elugoke, N. O. (2015). An assessment of

daytime surface urban heat island in Onitsha, Nigeria [Paper presentation]. National Metrological Society (NMetS) 2015 International Conference and 29th Annual General Meeting, Institute of Ecology and Environmental Studies, Obafemi Awolowo University, Ile-Ife, Nigeria. [Crossref]

Adewara, M. B., & Oyewole, A. M. (2019). Dynamic effects of urban heat island in Ilaro Town, Yewa South LGA of Ogun, South West Nigeria. *IOSR Journal of Environmental Science, Toxicology and Food Technology (IOSR-JESTFT), 13*(12), 51–60.

Akbari, H., Kolokotsa, D., & Santamouris, M. (2021). Cool roofs and pavements to mitigate urban heat islands. *Renewable and Sustainable Energy Reviews, 133*, 110296.

Babalola, O. S., & Akinsanola, A. A. (2016). Change detection in land surface temperature and land use land cover over Lagos Metropolis, Nigeria. *Journal of Remote Sensing & GIS, 5*(3), 1–7. [Crossref]

Bello, A. L. (1993). Kaduna State. In R. K. Udo & A. B. Mamman (Eds.), *Nigeria giant in the tropics—State surveys* (Vol. 2). Gabumo Publishers.

Changkua, S., Baoya, S., Wenjing, L., Lina, W., & Yangyang, L. (2025). Investigating the influence of land cover on land surface temperature. *Advances in Space Research, 75*(3), 2614–2631. [Crossref]

Curran, P. J., & Atkinson, P. M. (1998). Geostatistics and remote sensing. *Progress in Physical Geography, 22*, 61–78. [Crossref]

Cyril, K. E., Mwanret, G. D., & Emmanuel, C. U. (2019). Land-use and land-cover analysis of Kaduna South Local Government Area, Kaduna State, Nigeria. *American Journal of Environmental Protection, 8*(3), 62–71. [Crossref]

Fabrizi, R., Bonafoni, S., & Biondi, R. (2010). Satellite and ground-based sensor for the urban heat island analysis in the city of Rome. *Remote Sensing, 2*, 140–145. [Crossref]

Falahatkar, S., Hosseini, S. M., & Soffianian, A. R. (2011). The relationship between land cover changes and spatial-temporal dynamics of land surface temperature. *Indian Journal of Science, 4*(2), 76–80. [Crossref]

Ifatimehin, O. O. (2007). An assessment of urban heat island of Lokoja town and surroundings using Landsat ETM data. *FUTY Journal of the Environment, 2*(1), 9–17.

Isioye, O. A., Ikwueze, H. U., & Akomolafe, E. A. (2020). Urban heat island effects and thermal comfort in Abuja Municipal Area Council of Nigeria. *FUTY Journal of the Environment, 14*(2), 19–34.

Jacob, R. J. (2015). *Effects of urban growth on temporal variation of surface temperature in Katsina Metropolis, Nigeria* [Master's thesis, Ahmadu Bello University].

Mande, K. H., & Abashiya, D. O. (2020). Assessment of urban heat island in Kaduna Metropolis between 2000 and 2018. *FUDMA Journal of Sciences (FJS), 4*(4), 166–174. [Crossref]

Nantip, T. G., Obot, A. I., & Peter, A. O. (2023). Classification of land-use/land-cover in Kaduna Metropolis, Kaduna State, Nigeria. *Geoinfor Geostat: An Overview, 11*(5), 1–7.

NASA. (2015). *Landsat 8 science data users handbook*. United States. http://landsat.usgs.gov/landsat.php

Ngie, A., Abutaleb, K., Ahmed, F., Taiwo, O. J., Darwish, A. A., & Ahmed, M. (2015). An estimation of land surface temperatures from Landsat ETM+ images for Durban South Africa. *GeoTech Rwanda, 1*(1), 1–9. [Crossref]

Nigerian Meteorological Agency (NIMET). (2018). *Daily meteorological variables*.

Nigerian Meteorological Agency (NiMet). (2023). *Climate reports for Kaduna Metropolis*. https://nimet.gov.ng

Ogashwar, I., & Basto, V. (2012). A quantitative approach for analyzing the relationship between urban heat islands and land cover. *Remote Sensing, 4*, 3596–3618. [Crossref]

Oke, T. R., Mills, G., Christen, A., & Voogt, J. A. (2020). *Urban climates*. Cambridge University Press.

United States Geological Survey. (2016). *Landsat 8 (L8) data users handbook* (Version 2.0). Department of the Interior, United States Geological Survey, EROS.

Wuyep, S. Z., & Samuel, A. A. (2020). Assessment of urban heat island using remote sensing and GIS techniques in Jos Metropolis, Nigeria. *FUDMA International Journal of Social Sciences (FUDIJOSS), 2*(2), 29–40.

Yusuf, Y. Y., Garba, H., Mohammed, M. D., Abdullahi, U., Muhammad, U., Mohammed, A. A., & Auwal, H. A. (2023). Analysis of two decades variations in urban heat island using remotely sensed data in Nguru Local Government Area, Yobe State, Nigeria. *International Journal of Environment and Geoinformatics, 10*(2), 110–119. [Crossref]

Zahraddeen, I., Ibrahim, B. I., & Zachariah, A. (2016). Estimation of land surface temperature of Kaduna Metropolis, Nigeria using Landsat images. *Science World Journal, 19*(3), 36–41.

## APPENDIX 1

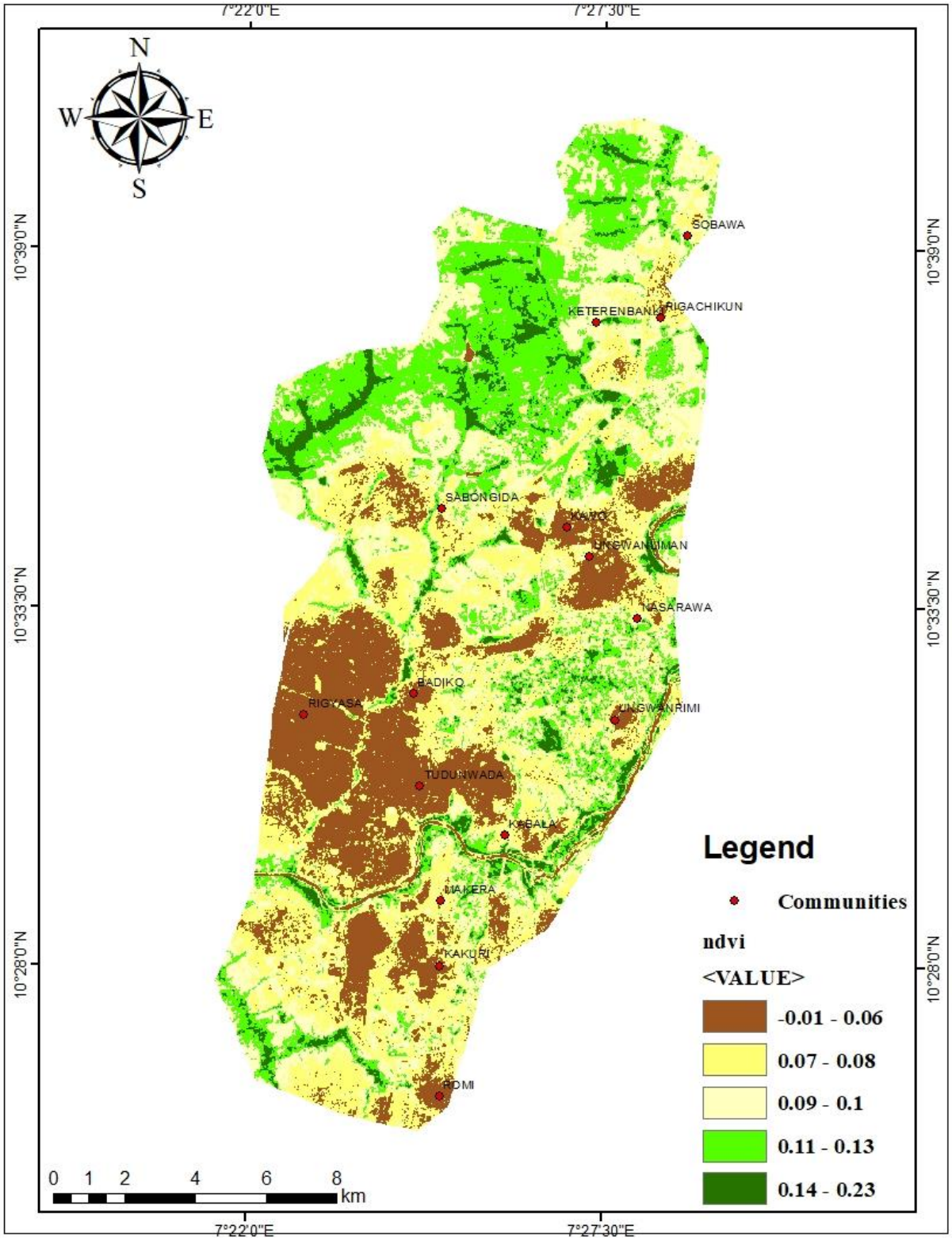


**NDVI of the Study Area**

## APPENDIX 2

**NDVI, LST, UHI AND AIR SURFACE TEMPERATURE(AT) VALUES OF SAMPLE POINTS**

| POINT | LATITUDE | LONGITUDE | NDVI | LST (°C) | UHI (°C) | AT (°C) |
|---|---|---|---|---|---|---|
| 1 | 10.571389 | 7.454722 | 0.059 | 30.66 | 6.44 | 30.16 |
| 2 | 10.5125 | 7.411111 | 0.043 | 30.67 | 6.48 | 30.07 |
| 3 | 10.653333 | 7.479722 | 0.075 | 30.81 | 6.88 | 30.21 |
| 4 | 10.583333 | 7.416667 | 0.085 | 30.73 | 6.66 | 30.33 |
| 5 | 10.45 | 7.366667 | 0.123 | 30.38 | 5.65 | 29.58 |
| 6 | 10.433333 | 7.416667 | 0.046 | 30.95 | 7.28 | 30.45 |
| 7 | 10.55 | 7.416667 | 0.044 | 30.69 | 6.54 | 30.19 |
| 8 | 10.530556 | 7.381111 | 0.039 | 30.81 | 6.95 | 30.11 |
| 9 | 10.6325 | 7.472778 | 0.085 | 30.29 | 5.38 | 29.59 |
| 10 | 10.6325 | 7.472778 | 0.085 | 30.29 | 5.38 | 29.59 |
| 11 | 10.6325 | 7.472778 | 0.085 | 30.29 | 5.38 | 29.59 |
| 12 | 10.6325 | 7.472778 | 0.085 | 30.29 | 5.38 | 29.79 |
| 13 | 10.565833 | 7.404722 | 0.054 | 30.44 | 5.83 | 29.88 |
| 14 | 10.6 | 7.45 | 0.066 | 31.17 | 7.92 | 30.47 |
| 15 | 10.433333 | 7.416667 | 0.046 | 30.95 | 7.28 | 30.45 |
| 16 | 10.555556 | 7.467222 | 0.086 | 30.65 | 6.42 | 30.05 |
| 17 | 10.555556 | 7.467222 | 0.086 | 30.65 | 6.42 | 30.05 |
| 18 | 10.5 | 7.383333 | 0.075 | 30.48 | 5.92 | 29.88 |
| 19 | 10.483333 | 7.383333 | 0.133 | 29.97 | 4.46 | 29.37 |
| 20 | 10.483333 | 7.416667 | 0.073 | 30.70 | 6.55 | 30.10 |
| 21 | 10.483333 | 7.383333 | 0.133 | 29.97 | 4.46 | 29.27 |
| 22 | 10.631111 | 7.456111 | 0.085 | 30.51 | 6.01 | 29.81 |
| 23 | 10.578889 | 7.448889 | 0.048 | 30.24 | 5.23 | 29.74 |
| 24 | 10.466667 | 7.416667 | 0.054 | 31.00 | 7.42 | 30.00 |
| 25 | 10.483333 | 7.416667 | 0.073 | 30.70 | 6.55 | 29.80 |
| 26 | 10.6 | 7.45 | 0.066 | 31.17 | 7.92 | 30.67 |
| 27 | 10.523056 | 7.440278 | 0.102 | 30.15 | 4.98 | 29.55 |
| 28 | 10.5 | 7.433333 | 0.082 | 30.19 | 5.11 | 29.59 |
| 29 | 10.433333 | 7.383333 | 0.065 | 30.83 | 6.94 | 30.33 |
| 30 | 10.483333 | 7.433333 | 0.054 | 30.65 | 6.43 | 29.95 |
| 31 | 10.536111 | 7.409444 | 0.047 | 30.63 | 6.36 | 29.93 |
| 32 | 10.571389 | 7.454722 | 0.059 | 30.66 | 6.44 | 30.26 |
| 33 | 10.554167 | 7.418889 | 0.046 | 30.68 | 6.49 | 30.18 |
| 34 | 10.548889 | 7.416944 | 0.043 | 30.62 | 6.34 | 30.12 |
| 35 | 10.546389 | 7.426667 | 0.064 | 30.54 | 6.10 | 29.94 |
| 36 | 10.5275 | 7.41 | 0.052 | 30.39 | 5.68 | 29.69 |
| 37 | 10.540833 | 7.3825 | 0.047 | 30.65 | 6.43 | 29.95 |
| 38 | 10.540278 | 7.473611 | 0.101 | 30.18 | 5.06 | 29.48 |
| 39 | 10.554722 | 7.473611 | 0.065 | 30.62 | 6.34 | 30.12 |
| 40 | 10.523056 | 7.462222 | 0.062 | 30.62 | 6.34 | 30.12 |
| 41 | 10.529722 | 7.461389 | 0.052 | 30.55 | 6.14 | 29.75 |
| 42 | 10.474167 | 7.433333 | 0.057 | 30.45 | 5.85 | 29.85 |
| 43 | 10.461944 | 7.427222 | 0.098 | 30.71 | 6.60 | 30.21 |
| 44 | 10.554167 | 7.441667 | 0.051 | 30.64 | 6.39 | 30.14 |
| 45 | 10.600282 | 7.380175 | 0.143 | 29.37 | 2.74 | 28.77 |
| 46 | 10.630191 | 7.435947 | 0.143 | 30.29 | 5.38 | 29.49 |
| 47 | 10.616076 | 7.397411 | 0.131 | 30.18 | 5.06 | 29.68 |
| 48 | 10.486367 | 7.405308 | 0.010 | 29.54 | 3.22 | 28.64 |
| 49 | 10.505675 | 7.460621 | 0.022 | 28.80 | 1.10 | 28.30 |
| 50 | 10.675052 | 7.463162 | 0.128 | 30.32 | 5.46 | 29.82 |
| 51 | 10.660109 | 7.460044 | 0.117 | 30.46 | 5.88 | 29.46 |
| 52 | 10.568193 | 7.409733 | 0.079 | 30.93 | 7.21 | 30.43 |
| 53 | 10.523593 | 7.446029 | 0.147 | 30.71 | 6.60 | 29.81 |
| 54 | 10.452569 | 7.383258 | 0.091 | 31.04 | 7.53 | 30.54 |
| 55 | 10.46979 | 7.364221 | 0.083 | 30.90 | 7.14 | 30.00 |
| 56 | 10.603328 | 7.413421 | 0.079 | 31.26 | 8.18 | 30.76 |
| 57 | 10.657629 | 7.481242 | 0.065 | 30.45 | 5.85 | 29.85 |
| 58 | 10.458325 | 7.405172 | 0.070 | 31.22 | 8.04 | 30.72 |
| 59 | 10.539596 | 7.450783 | 0.128 | 30.01 | 4.57 | 29.01 |
| 60 | 10.656943 | 7.419915 | 0.095 | 30.66 | 6.45 | 30.16 |

## APPENDIX 3

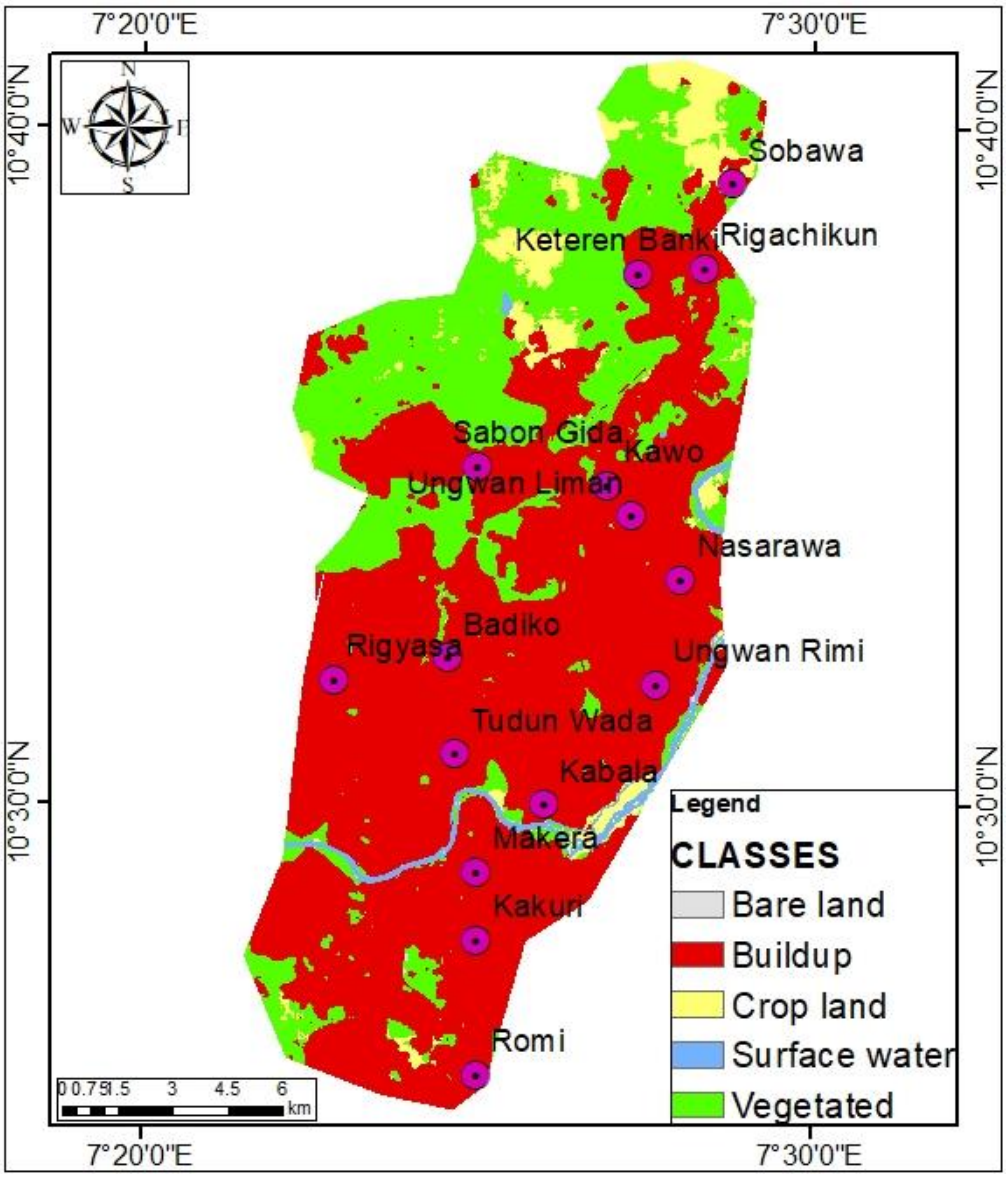


**Land Use – Land Cover of the Study Area**